J Mater Sci (2008) 43:3589–3595
DOI 10.1007/s10853-008-2567-4

# Electrochemical impedance study of TiAlN film coating on a Ni-based alloy in 0.9% NaCl

**K. T. Liu · J. G. Duh**

Received: 9 July 2007 / Accepted: 19 February 2008 / Published online: 29 March 2008


**Abstract** TiAlN films were deposited on Ni-based alloy by RF sputtering technique. Electrochemical impedance spectroscopy was employed as in situ technique to investigate the evolution of the TiAlN films on exposure in biological media. After immediate- to short-term exposure, the biological media was further evaluated with inductively coupled plasma-atomic emission spectrometer (ICP-AES) to measure the release of metal ions, such as nickel. The results of ICP-AES analysis showed that TiAlN coated on a Ni-based alloy effectively reduced metal ion release levels, as compared to the uncoated Ni-based alloy. The effect of the nitride films was also reflected in corrosion resistance and the corrosion rate. It was demonstrated that the TiAlN-coated Ni-based alloy revealed a higher corrosion resistance than uncoated substrates. Furthermore, the impedance of nitride films on a Ni-based alloy was larger than that of the metal's charge transfer reaction at short-term immersion.

## Introduction

In biomedical applications, conventional nickel-based alloys have historically exhibited an acceptable combination of strength, hardness, and wear resistance in vivo [1, 2]. Although nickel-based alloys have been successfully developed for long time, there are concerns with respect to the release of metal ions such as Ni and Be from alloys to adjacent tissues [3, 4]. At excessive concentrations, the ionic substances such as Ni, Co, Be, and many others can give rise to toxic symptom and hypersensitivity in human beings [5–7]. In fact, the problem of element released into body was affected significantly by corrosion process.

Recently, the nitride coatings have been developed broadly in many applications due to its thermal conductivity, excellent corrosion and wear resistance, and superior hardness [8–13]. Titanium–aluminum nitride (TiAlN) is a metastable material and could be synthesized through reactive physical vapor deposition methods [14]. A significant increase in the wear resistance of steel and hard metal alloy when coated with TiAlN was observed [15]. Recently, a novel TiAlN film processing technique was developed and successfully applied in fabrication of metal-ceramic restorations [2].

Electrochemical impedance spectroscopy (EIS) is a powerful analysis technique to derive extensive information, including corrosion reactions, mass transfer, electrical charge transfer characteristics, and double-layer configurations of physical vapor deposition (PVD) coating layers [16–20]. The purpose of this study was to investigate the feasibility of achieving better corrosion properties in the dental alloys with nitride films. In addition, the polarization resistance and double-layer capacitance were studied to quantitatively evaluate the corrosion resistance of coatings. To further extend the coatings' application in biomaterial, the coatings' characteristics were evaluated and discussed.

## Experimental procedures

A commercially available nickel-based dental alloy: Ticonium™ (Lot No. 072303, Ticonium Company, Division of CMP Industries LLC, Albany, NY) with compositions of 63 w/o Nickel, 16 w/o Chromium, 8 w/o Cobalt, 5 w/o

K. T. Liu · J. G. Duh (✉)
Department of Material Science and Engineering,
National Tsing-Hua University, Hsinchu 300, Taiwan
e-mail: jgd@mx.nthu.edu.tw

Molybdenum, 3.5 w/o Manganese, 3 w/o Aluminum, and 1.5 w/o Beryllium was used in this study. Disc specimens with 1.5 mm in thickness and 12.0 mm in diameter were cut from the original ingot with Buehler Isocut® (Buehler Ltd. Lake Bluff, IL). The disc surfaces were metallurgically ground with silicone carbide sandpapers (Buehler Ltd. Lake Bluff, IL) to grip 1,200 and then further polished with 1.0 μm aluminum powder (Micropolish 1.0 micro alpha aluminum, Buehler Ltd. Lake Bluff, IL) slurry and used as controls. TiAlN films were deposited by reactive radio frequency (RF) magnetron sputter deposition system onto specimen surfaces [21]. The deposition temperature was 300 °C and the deposition rate was 5.56 nm/min. The nitride film coatings were accomplished with deposition pressure of $4.6 \times 10^{-3}$mbar for 3 h. The direct current offsets of titanium and aluminum targets were −550 and −220 volts, respectively. At the completion of nitride film coatings on the polished discs, the working chamber was vented and bench cooled to room temperature. The TiAlN-film-coated specimens were assigned as TiAlN-film-coated group. The tested surface area was estimated to be 1.5 $cm^2$ and the thickness of the nitride film was measured to be approximately 1 μm. The composition of TiAlN films was analyzed by an electron probe microanalyzer (EPMA, JXA-8800M, JEOL, Tokyo, Japan). The acceleration voltage of the electron gun was adjusted at a level of 8 kV. The phase and crystal structure of the films were identified by an X-ray diffraction analyzer (Mxp18, MAC Science, Yokohama, Japan), using the grazing-incidence technique. The X-ray generator was 18 kW rotating Cu anode, operated at 40 kV and 150 mA. The $2\theta$ scanning range was from 30° to 80°s. Electrochemical impedance spectroscopy (EIS) measurement was performed by EIS 300 System (Gamry Instrument, Warminster, PA). The electrolyte used for the EIS measurements was 0.9 w/o NaCl solution with seven immersion periods including base line, 1, 12, 48, 96, 120, and 144 h time points. Saturated calomel electrode (SCE) and carbon rod were used as the reference electrode and counterelectrode, respectively. The EIS measurements were carried out at open-circuit potential in the frequency from 0.01 Hz to 100 kHz with a perturbation amplitude of 10 mV. The EIS tests were carried out in triplicate to evaluate reproducibility. Besides, the stabilization potential $E_0$ was applied for 60 min before recording the impedance spectrum. In all cases this time is sufficient to attain a well-defined steady state.

After EIS measurements, a field emission scanning electron microscope (FESEM, JSM-6500, JEOL, Tokyo, Japan) was used to observe the surface morphology of tested specimens. The concentration of leached elements in electrolyte during EIS measurements was analyzed with an inductively coupled plasma-atomic emission spectrometer (ICP-AES, Perkin Elmer, Optima 3000DV, USA). The depth profiles of TiAlN film were measured by Auger electron spectroscopy (AES Auger 670 PHI Xi, Physical Electronics).

## Results and discussion

### Surface analysis

The X-ray diffraction pattern of TiAlN film is represented in Fig. 1. The structure of TiAlN was identified as the B1-NaCl cubic type, similar to pure TiN. Peak intensity of (111) and (200) were comparable to each other due to the addition of aluminum element. If the concentration of aluminum in TiAlN system, $x$, exceed 0.65 in $Ti_{1-x}Al_xN$ system, the phase was reported to be changed from cubic B1 type to hexagonal B4 type [22]. In this study, the composition of the as-deposited $Ti_{1-x}Al_xN$ coating was measured by EPMA in combination with the ZAF correction and deconvolution method [23]. The stoichiometric value of $x$ in the $Ti_{1-x}Al_xN$ coatings was evaluated to be 0.25. Therefore, the pattern of TiAlN structure revealed the B1 type rather than B4 type, as indicated in Fig. 1.

### Electrochemical properties

Electrochemical impedance spectroscopy (EIS) is useful to investigate electrochemical behavior of corrosion process without damage to the sample. The EIS measurements were used to determine corrosion properties of surface coating layer. Figures 2 and 3 present the impedance spectrum of control and TiAlN-film-coated surfaces, respectively. From the Nyquist diagram, the electrolyte resistance at high frequencies was obtained. The electrolyte resistance revealed a low resistance around 30 Ω $cm^2$ due to the presence of chloride and sodium ions in solution. In the early immersion test, the resistance of Ni-based alloy was large. Therefore, a solid line could be drawn at an angle of 45° to the horizontal axis in Fig. 3b, which is characteristic of diffusion across the oxide layer on the Ni-based layer in the low-frequency region [16, 27].

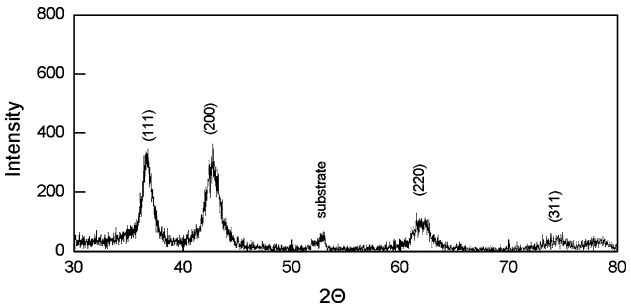


**Fig. 1** X-ray diffraction of as-deposited TiAlN

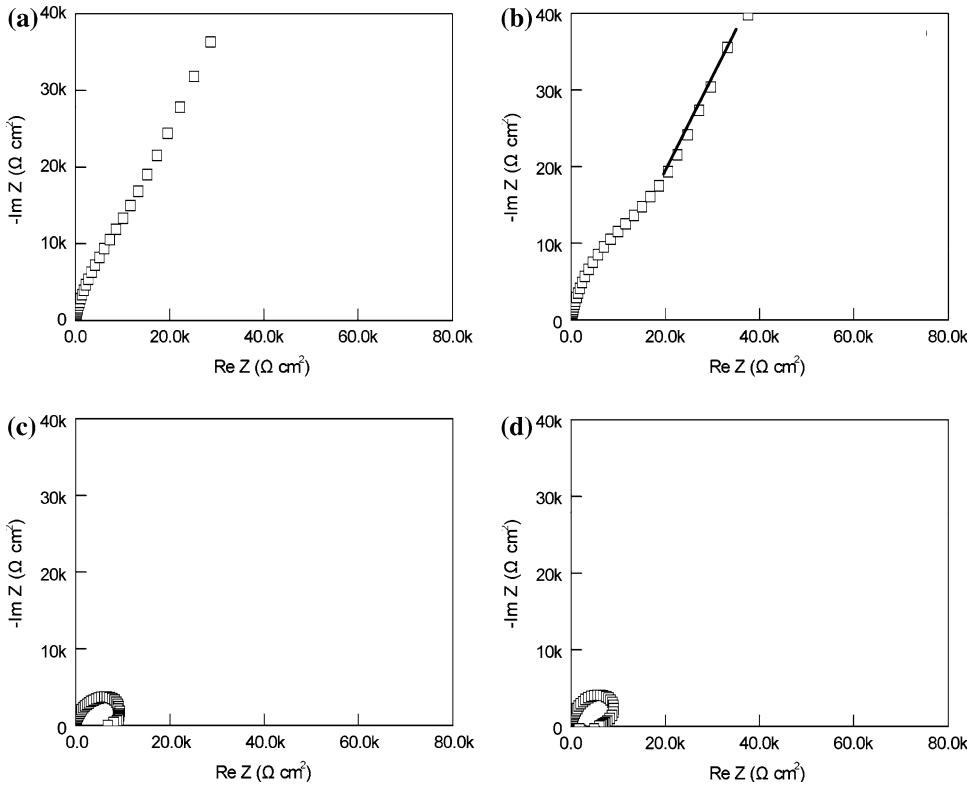


**Fig. 2** Impedance spectra of Ni-based alloy for various immersion times (**a**) 0 h, (**b**) 12 h, (**c**) 48 h, and (**d**) 144 h

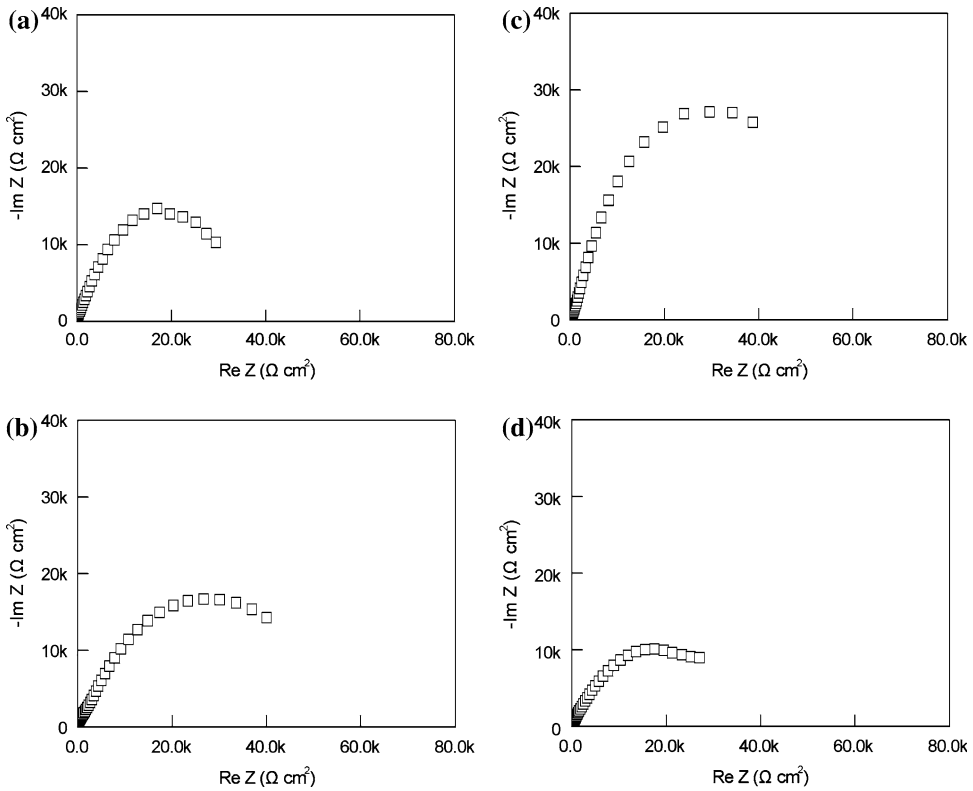


**Fig. 3** Impedance spectra of TiAlN film for various immersion times (**a**) 0 h, (**b**) 12 h, (**c**) 48 h, and (**d**) 144 h

With increasing immersion time, the impedance curve of Ni-based alloy changes from linear to circular due to oxide layer breakdown. Owing to the aggressive $Cl^-$ ion attacking, pitting corrosion can form and this process is deduced from the presence of an inductive loop in the Nyquist plots. The semicircles observed in the Nyquist plot

for TiAlN specimens were mostly described to the presence of surface nitride film [16, 18]. Consequently, the polarization resistance values obtained from the Nyquist plots could be employed to evaluate the corrosion resistance of nitride film.

The polarization resistance was calculated by extrapolation of the low semicircle at low frequencies. From equivalent circuit analysis, the complex impedance $Z$ [25] is given by:

$$Z = R_s + \frac{R_p}{1 + j\omega R_p C_{dl}} \quad (1)$$

where $\omega$ is the angular frequency, $\omega = 2\pi f$, $R_s$ is the solution resistance, and $C_{dl}$ is the double-layer capacitance.

Separation of $Z$ into real and imaginary components gives:

$$Z_{real} = R_s + \frac{CR_p}{1 + \omega^2 C^2 R_p^2} \quad (2)$$

$$Z_{img} = \frac{\omega C R_p^2}{1 + \omega^2 C^2 R_p^2} \quad (3)$$

According to these equations, the polarization resistance was measured for different immersion times, as shown in Fig. 4. It was revealed that the polarization resistance of Ni-based alloy dramatically decreased at early immersion time and then reached steady state at 48 h. The polarization resistance of TiAlN film increased at 12 h and maintained steady state of 37 kΩ cm$^2$ until 144 h of immersion. The resistances of Ni-based alloy and TiAlN film are listed in Table 1.

In general, the double-layer capacitance in the parameter includes natures of layers, such as composition and the number of charge transferred. Thus, the parameter $C_{dl}$ coupled with $R_p$ is the resistance of corrosion process with respect to the charge-transfer reaction between interface of the material and electrolyte. For a non-ideal impedance response, the capacitance (C), modified by a constant phase element (Q), is defined as [26]:

$$Q = Z_{cpe} = C^{-1}(j\omega)^{-n} \quad (4)$$

For $n = 1$, the Q element reduced to a capacitor with a capacitance C, and for $n = 0$, it is a simple resistor. In general, the impedance of surface nitride film can be a passive film; so, the charge transfer reaction of nitride film is relatively small and can be ignored.

The capacitance of Ni-based alloy increased with immersion time and finally reached the near steady state, as indicated in Fig. 5a. For TiAlN film, the capacitance exhibited two steps, as shown in Fig. 5b. In the first step, the capacitance decreased from 7 h to 12 h, while there was an order of magnitude increase from 120 h to 144 h in the second step. Capacitances of Ni-based alloy and TiAlN film are listed in Table 2. Based on the measurement of resistance and double-layer capacitance, the electrochemical behavior of TiAlN film in 0.9% NaCl solution can be simulated by equivalent circuits. Figure 6a includes theoretical solution resistance ($R_{sol}$), and the resistance and

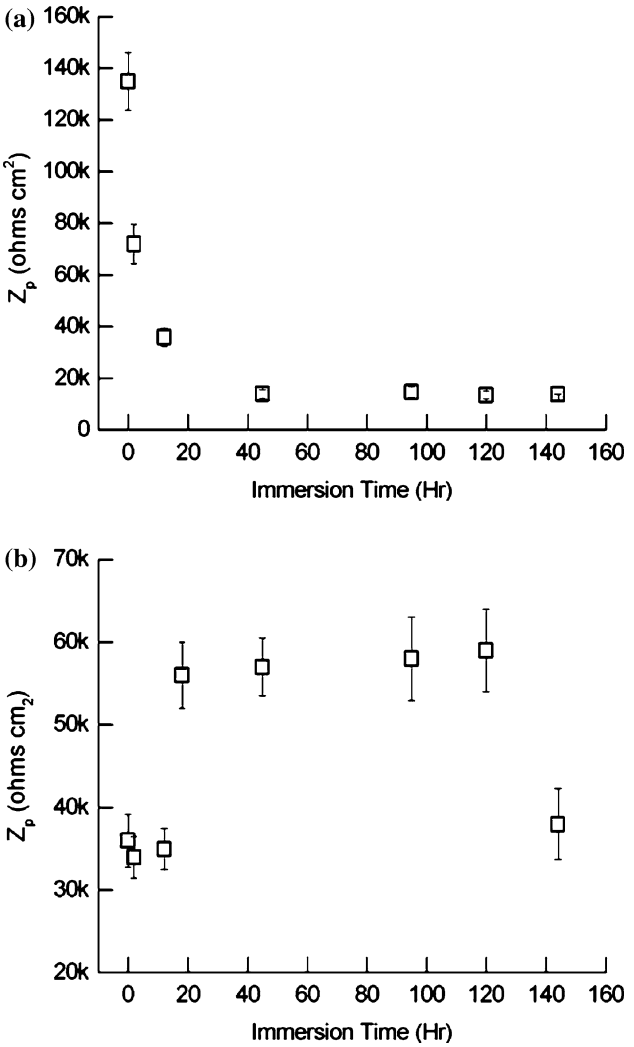


**Fig. 4** Impedance Zp value versus immersion time for (**a**) Ni-based alloy and (**b**) TiAlN

**Table 1** Polarization resistance of Ni-based alloy and TiAlN film for different immersion times

| Immersion time (h) | Ni-based alloy (Ω cm$^2$) | TiAlN film (Ω cm$^2$) |
|---|---|---|
| 0 | 130,400 | 35,400 |
| 1 | 70,600 | 31,900 |
| 12 | 34,100 | 51,900 |
| 48 | 11,800 | 57,100 |
| 96 | 12,100 | 56,900 |
| 120 | 11,200 | 56,900 |
| 144 | 10,800 | 37,200 |

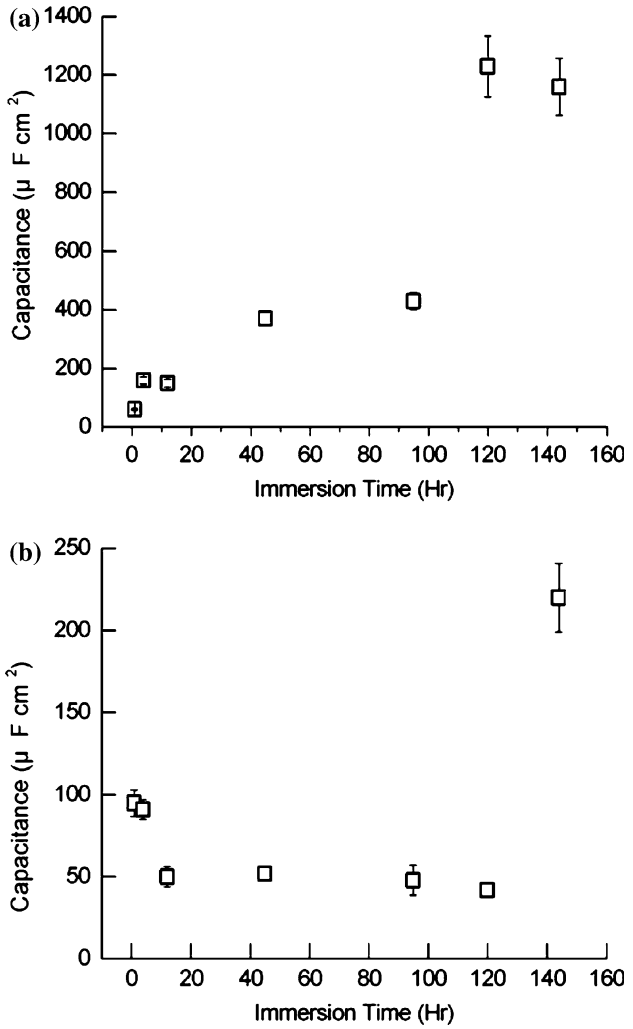


**Fig. 5** Capacitance value versus immersion time for (**a**) Ni-based alloy and (**b**) TiAlN

capacitance for nitride film ($R_{ni}$ and $C_{ni}$). The protective nitride film might provide the better corrosion resistance in 0.9% NaCl solution. Therefore, the influence of charge transfer reaction in TiAlN film might be negligible on the impedance data.

In early immersion time, the uncoated Ni-based alloys represented nearly large semicircle corresponding to the decayed oxide film, as shown in Fig. 3a and b. This means two time constants associated to the oxide film and charge transfer reaction occurred simultaneously [24, 27]. The equivalent circuit in early immersion time was proposed in Fig. 6b, including the charge transfer resistance ($R_{ct}$), double layer capacitance ($C_{dl}$), oxide resistance ($R_{ox}$), and oxide capacitance ($C_{ox}$). With increasing immersion time, the effect of charge transfer reaction on the impedance data was obviously enhanced, as indicated in Fig. 3c and d. This corrosion behavior showed that the oxide film was severely attacked by fluoride ions, and the number of

**Table 2** Capacitance of Ni-based alloy and TiAlN film for different immersion times

| Immersion time (h) | Ni-based alloy (F cm$^2$) | TiAlN film (F cm$^2$) |
|---|---|---|
| 0 | 9.68E-05 | 8.97E-05 |
| 1 | 1.40E-04 | 8.42E-05 |
| 12 | 1.29E-04 | 5.06E-05 |
| 48 | 3.38E-04 | 5.01E-05 |
| 96 | 4.46E-04 | 5.07E-05 |
| 120 | 1.24E-03 | 3.35E-05 |
| 144 | 1.14E-03 | 2.28E-04 |

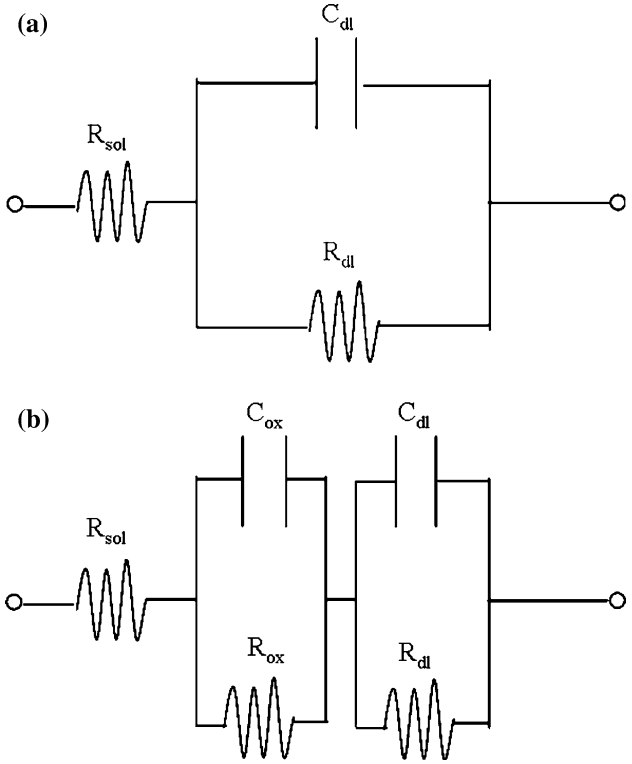


**Fig. 6** Equivalent circuits in 0.9% NaCl solution for (**a**) TiAlN film and (**b**) Ni-based alloys

charges accumulated on the surface indicated the charge transfer reaction.

## Surface morphology and dissolved analysis

After 144h immersion in 0.9-wt.% NaCl solution, Ni-based alloy revealed dramatic damages. Cracks showed up on the surface due to corrosion, as indicated in Fig. 7a. The corrosion rate increased rapidly and the capacitance of double-layer apparently increased, too. The TiAlN film exhibited the pitting holes around ten micrometers, as shown in Fig. 7b. In this study, TiAlN film onto the Ni-based alloy, the only channel, where corrosion electrolyte transferred to the deeper position, acted as the major factor that

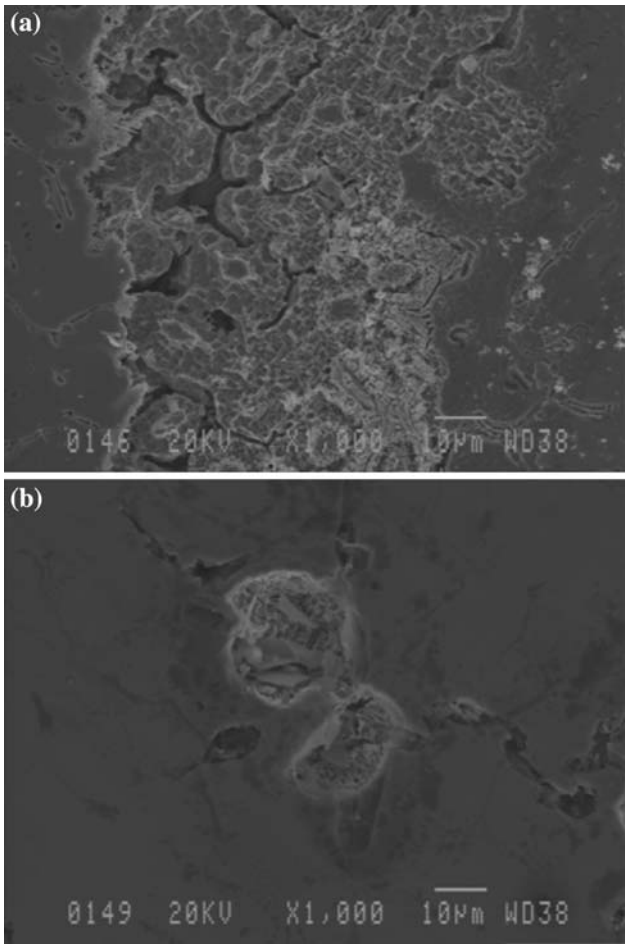


**Fig. 7** SEM morphologies after 144 h immersion for (**a**) Ni-based alloy and (**b**) TiAlN

determine the corrosion resistance of coating. Pitting corrosion occurred at this site. The Ni-based alloy showed severe pitting corrosion on the surface after 144-h immersion test. Thus, the amount of dissolved nickel in the Ni-based alloy increased with immersion time, as shown in Fig. 8.

In EIS spectrum, the resistance of Ni-based alloy reached the lowest at 48 h. The dissolved concentration for Ni-based alloy suddenly increased after 48 h corresponding to the resistance of Ni-based alloy, which revealed the lowest resistance for 48 h. For TiAlN film onto Ni-based alloy, the dissolution of Ni, Ti, and Al elements was not detected in the electrolyte by the ICP-AES. In fact, after long-term immersion test, the TiAlN film effectively blocked the dissolution of Ni in the electrolyte.

The depth profile of TiAlN film onto Ni-based alloy after 144 h is indicated in Fig. 9. The concentration of oxygen accumulated on the surface and then decreased with sputtering time. When the corrosion electrolyte reached this pitting site, Al dissolved and aluminum hydroxide formed. Because the corrosion process was

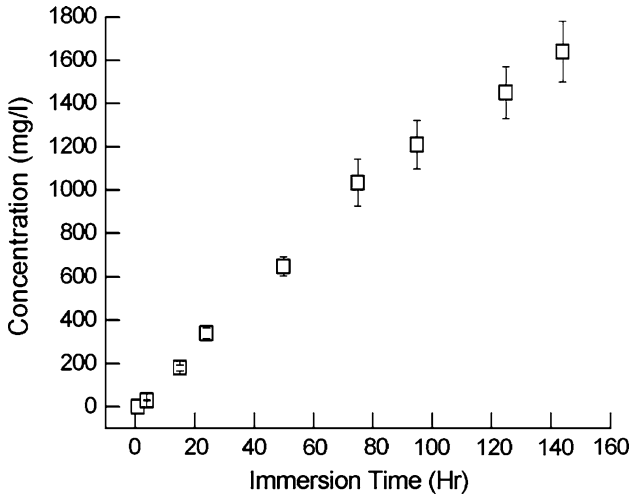


**Fig. 8** Dissolved concentration of nickel in Ni-based alloy

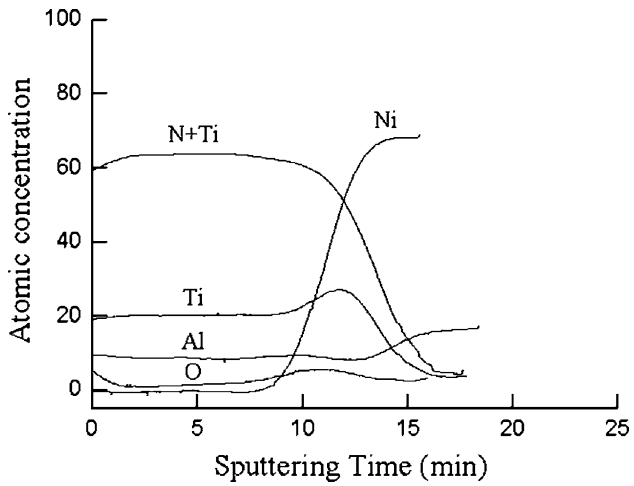


**Fig. 9** Depth profile of TiAlN film after 144-h immersion

obstructed between the coating and substrate due to the corrosion product of aluminum hydroxide, the self-repairing function took place in the TiAlN film.

## Conclusions

1. TiAlN film was successfully deposited onto Ni-based dental alloy by R.F. sputtering to improve corrosion resistance. The coating layers exhibited smoother surface, as compared to Ni-based dental alloys.
2. During long-term immersion test, polarization resistance of TiAlN film was raised and larger than that of Ni-based dental alloys. The capacitance of TiAlN film was an order of magnitude less than Ni-based dental alloys. Therefore, the TiAlN film can be effectively used in oral cavity without serious corrosive damage.

3. After 144-h immersion test, Ni-based alloys showed ion release in the electrolyte. With TiAlN film covered on the Ni-based dental alloys, the ions released such as nickel, titanium, and aluminum, were not detected in the electrolyte. It was demonstrated that TiAlN film was an effective barrier onto Ni-based dental alloy and acted to block the ions transferred from the substrate.
4. The surface morphology of TiAlN film exhibited only slight pitting corrosion, with the protective oxide film formed on the surface after immersion test. In contrast, the surface morphology of Ni-based dental alloys showed dramatic damage due to the aggressive $Cl^-$ ion attack in the corrosive test.

**Acknowledgements** This work is supported by Center for Nano-Science and Technology of the University System of Taiwan, Taiwan under Project No. 91B0502J4. Partial support from National Science Council under the contract No. NSC 93-2216-E-007-035 is also appreciated.

## References

1. Raimondi MT, Pietrabissa R (2000) Biomaterials 21:907
2. Chung KH, Duh JG, Shin D, Cagna DR, Cronin R (2002) J Biomed Mater Res 63:516
3. Covington JS, McBride MA, Slage WF, Disney AL (1985) J Prosthet Dent 54:127
4. Schmalz G, Garhammer P (2002) Dent Mater 18:396
5. Hornez JC, Lefevre A, Joly D, Hildebrand HF (2002) Biomole Eng 19:103
6. Brown SS, Savory J (1979) Chemical toxicology and clinical chemistry of metals. Raven, New York
7. Cangul H, Broday L, Salnikow K, Sutherland J, Peng W, Zhang Q, Poltaratsky V, Yee H, Zoroddu MA, Costa M (2002) Toxic Lett 127:69
8. Piscanec S, Ciacchi LC, Vesselli E, Comelli G, Sbaizero O, Meriani S, Vita AD (2004) Acta Mater 52:1237
9. Casaletto MP, Ingo GM, Kaciulis S, Mattogno G, Pandolfi L, Scavia G (2001) Appl Surf Sci 172:167
10. Mossman T (1983) J Immunol Methods 65:55
11. Liu KT, Duh JG, Chung KH, Wang JH (2005) Surf Coat Tech 200:2100
12. Oss CJV, Chaudhury MK, Good RJ (1988) Chem Rev 88:927
13. Young T (1905) Philos Trans R Soc London 95:65
14. Choi IS, Park CJ (2000) Surf Coat Technol 131:385
15. Bressan JD, Hesse R, Silva EM (2001) Wear 250:561
16. Carnot A, Frateur I, Zanna S, Tribollet B, Brugger ID, Marcus P (2003) Corr Sci 45:2513
17. Piippo J, Elsener B, Bohni H (1993) Surf Coat Technol 61:43
18. Rudenja S, Leygraf C, Pan J, Kulu P, Taliimets E (1999) Surf Coat Technol 114:124
19. Sun D, Monaghan P, Brantley WA, Johnston WM (2002) J Mater Sci: Mater Med 13:435
20. Sun D, Monaghan P, Brantley WA, Johnston WM (2002) J Mater Sci: Mater Med 13:443
21. Manso M, Ogueta S, Rigueiro JP, Garcia JP, Martinez-Duart JM (2002) Biomol Eng 19:239
22. Zhou M, Makino Y, Nose M, Nogi K (1999) Thin Solid Films 339:203
23. Goldstein JI (2003) Scanning electron microscopy and X-ray microanalysis. Plenum Press, New York
24. Kelly RG, Scully JR, Shoesmith DW, Buchheit RG (2003) Electrochemical techniques in corrosion science and engineering. Marcel Dekker, New York
25. Raistrick ID, Macdonald JR, Franceschetti DR (1987) Impedance spectroscopy emphasizing solid materials and systems. Wiley, New York
26. Huang HH (2003) Biomaterials 24:1575
27. Huang HH (2002) J Biomed Mater Res 60:458